Draft version December 11, 2016
Preprint typeset using LaTeX style AASTeX6 v. 1.0

HW 05: IMAGE PHOTOMETRY

Bryan Yamashiro[1] and Bryant Higa[2]
University of Hawaii at Manoa
2500 Campus Road
Honolulu, HI 96822

1. INTRODUCTION

The variable represent another kind of unusual star. As in the case of the peculiar stars, the variables are normal stars in special stages of their lifetimes, where particular combinations of atmospheric pressure and ionization conditions produce instabilities that cause the pulsations (Snow (1984)).

Evidence of the variability of Young Stellar Object (YSO) J161420.3-190648 (J-star,$\star$), a T Tau-type star, is discussed in this study. J-star is characterized as a classical T Tauri star (CTTS) which exhibit variability in stochastic light curves (Cody et al. (2014)). J-star, located at RA/Dec 16h 14m 20.3s -19d 06m 48.1s, features a literature R-magnitude of 13.2 and a K5 spectral type (Preibisch (2008)). The young T Tauri stars show variations on timescales of minutes to years, but vary from object to object (Gham et al. (1995)).

The variability of object J-star, was determined by analyzing the magnitude over time. J-star was compared to a standard star (J-standard,†), 16h 14m 20.912s -19d 06m 04.70s, which has a literature apparent R-magnitude of 13.5. Measurements were carried out on a set of nine images of varying dates and times. Each image contains fully reduced observations in R from the Las Cumbres Observatory Global Telescope (LCOGT) 1 m telescope network.

2. RELEVANT EQUATIONS

The flux of both J-star ($F_\star$) and J-standard ($F_\dagger$), provided in equation 1, were obtained with background subtraction, while also taking the gain (ξ) into account. The total counts of photons ($N_{\star,\dagger}$) from the star apertures were subtracted with the total background photon counts (B).

$$F_{\star,\dagger} = (N_{\star,\dagger} \times \xi) - B\xi \tag{1}$$

The error associated with the flux required the same inputs as the flux, with a few additional parameters. The new parameters included the number of pixels within the aperture (N_{px}), read noise (R), and the standard deviation of the mean Bξ component ($\sigma_{\overline{B\xi}}$).

$$\sigma_{F_{\star,\dagger}} = \sqrt{\frac{N_{\star,\dagger}}{\xi} + N_{px}(B\xi + R_{DN}^2) + N_{px}^2\sigma_{\overline{B\xi}}^2} \tag{2}$$

The *magnitude difference*, provided in equation 3, shows the magnitude and flux relationship between two stars. The apparent magnitude of J-star ($m_\star$) and the known magnitude of J-standard ($m_\dagger$) were both utilized. The equation also includes the flux ratio of both the photon fluxes $F_\star$ and $F_\dagger$. The error associated with the magnitude difference is provided in equation 4.

$$m_\star = -2.5\log_{10}\left(\frac{F_\star}{F_\dagger}\right) + m_\dagger \tag{3}$$

$$\delta m_\star = \sqrt{\left(\frac{\partial m_\star}{\partial F_\star}\delta F_\star\right)^2 + \left(\frac{\partial m_\dagger}{\partial F_\dagger}\delta F_\dagger\right)^2} \tag{4}$$

3. PROCEDURE AND OBSERVED QUANTITIES

3.1. *Background Measurements*

Initially, a defined background for each image was processed. An aperture background point was set to a specific location, and a square aperture of 60x60 pixels was generated around the point. The portion of the image with low amounts of bright species was chosen through analyzing the image with contour levels, shown in figure 1. The background was arbitrarily defined as the 60x60 pixel aperture flux region that produced a standard deviation of less than 18. The aperture background point was set to 16h 14m 17.0692s -19d 05m 50.3571s for the first parsed image. Subsequently, the background apertures for all following images were automatically set through coordinate transforms of the initial background point.

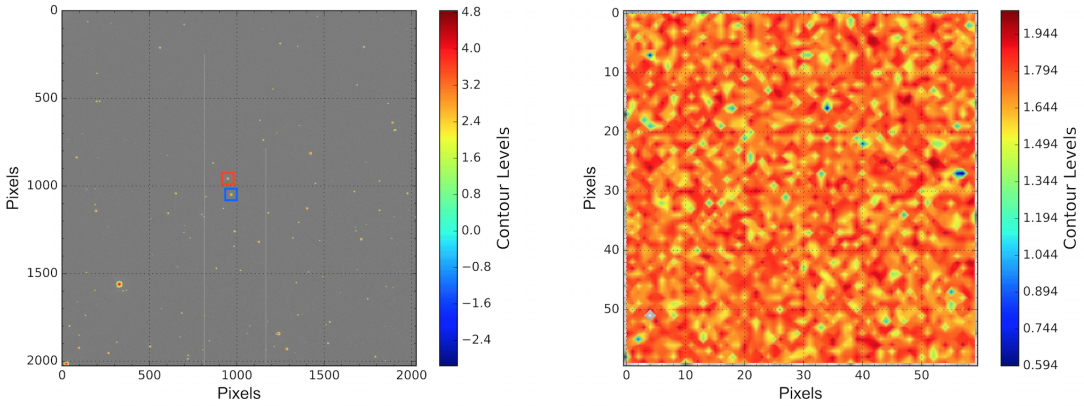

Figure 1. **Left:** The entire sky image shown with the boxed aperture regions of J-star (blue), J-standard (red), and the background (green). **Right:** The aperture region for the background image within the full-sky image. Note that the contour scales are used as a first approximation of finding a low intensity region before statistics are applied.

3.2. *J-star and J-standard Measurements*

The apertures for J-star and J-standard were generated through the same method as the background aperture. The aperture points for J-star and J-standard were 16h 14m 20.3s -19d 06m 48.1s and 16h 14m 20.912s -19d 06m 04.70s, respectively. The aperture dimensions for J-star and J-standard were set to 40x40 pixels, as this set of dimensions enclosed most of the high intensity contour levels of each star. The flux of both J-star and J-standard were measured through the dimensionally defined apertures, shown in figure 2.

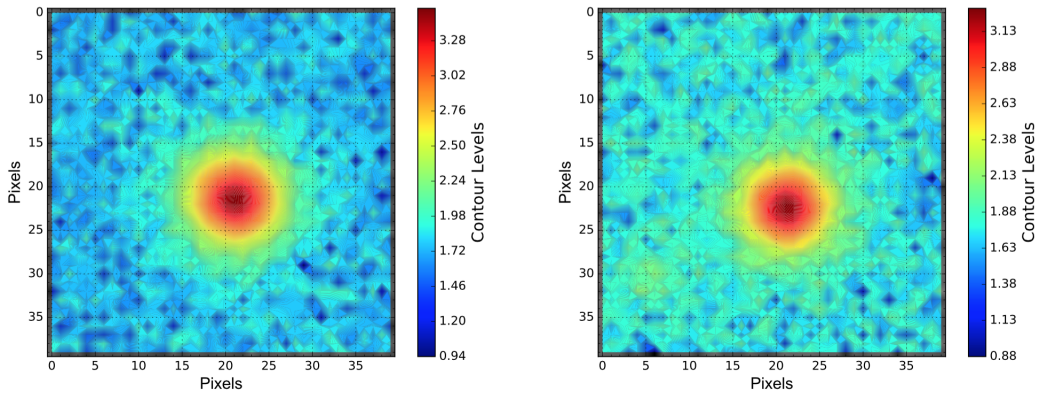

Figure 2. The photometric apertures containing both J-star (left) and J-standard (right). The contour levels are provided to observe the aperture localized intensities of both stars.

Table 2. Apparent Magnitude Data

Observation Number	Date [YYYY-mm-dd]	Observation Start [UT]	Observation Site ID	$F_\star$	$F_\dagger$	$m_\star$
1	2014-05-26	08:28:40	*cpt*	7940.341 ± 561.242	17379.420 ± 567.217	14.350 ± 0.085
2	2014-05-26	08:37:51	*cpt*	6813.614 ± 566.692	17511.252 ± 573.394	14.525 ± 0.097
3	2014-06-07	07:55:38	*cpt*	101939.352 ± 659.018	79653.540 ± 646.828	13.232 ± 0.011
4	2014-06-07	14:27:58	*elp*	80274.873 ± 711.150	79750.813 ± 710.887	13.493 ± 0.014
5	2014-06-07	22:19:14	*coj*	152179.862 ± 725.397	90519.662 ± 694.375	12.936 ± 0.010
6	2014-06-07	22:33:39	*coj*	112276.488 ± 777.333	95102.906 ± 769.403	13.320 ± 0.012
7	2014-06-07	22:34:10	*coj*	116910.639 ± 770.964	98636.746 ± 762.452	13.315 ± 0.011
8	2014-06-23	16:14:55	*lsc*	129502.242 ± 783.233	201560.828 ± 827.958	13.980 ± 0.008
9	2014-06-25	15:59:51	*lsc*	135379.422 ± 817.565	239263.188 ± 878.804	14.118 ± 0.008

NOTE—The times and dates represent the start of the observations. The flux measurements of J-star and J-standard were determined through aperture photometry. Magnitudes of J-star determined from magnitude and flux relationships are reported.

4. RESULTS

The various flux and apparent R-magnitude aperture photometry measurements for each of the nine images are provided in table 2 and presented in figure 3. The time varying magnitudes of J-star was found utilizing equation 3 and the appropriate values in table 2.

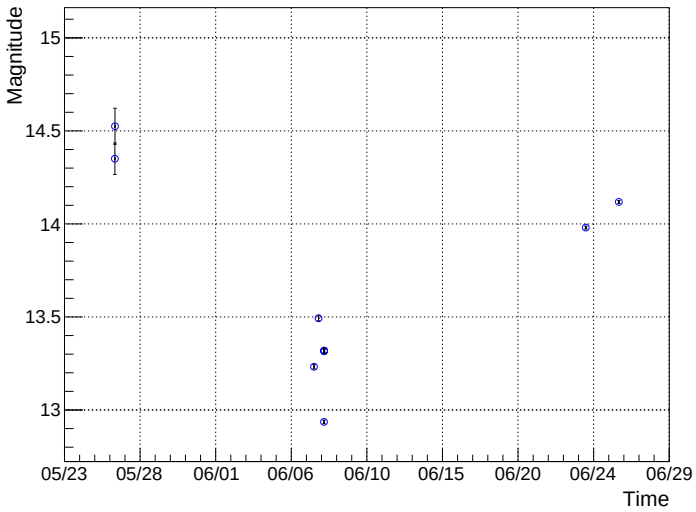

Figure 3. Magnitude diagram of J-star over approximately a month timescale. Note that observations 5 and 6 are similar in time and magnitude, therefore the points are essentially overlapping.

5. DISCUSSION

The J-star magnitude, shown in figure 3, clearly exhibits variability between approximately 13 to 14.5 magnitudes. The R-magnitude literature of 13.2 lies within this magnitude range. It is imperative to note that without additional data on a larger time range, it is impossible to definitively determine the variability of J-star. Multiple periods of the magnitude fluctuation would solidify the variability conjecture. The change in magnitude slightly followed characteristics of CTTS, as CTTS species were determined to portray rotation periods of approximately 2.8 days (Herbst (2012)).

J-star could more accurately be classified as an irregular variable suffering occultations (Type III variable) with the

information provided in the study. Earlier type CTTS are thought to undergo irregular variability with brightness drops from 1 to 3 magnitudes followed by irregular recoveries. (Herbst (2012)). This characteristic is evident in figure 3, if the maximum magnitude is taken around 14.5 and the minimum magnitude is taken around 13. This assumption assumes that the period from the maximum to the minimum is approximately 14 days. Converse to the above statement, the assumption does not fully support the 2.8 day period mentioned by common CTTS objects, as the period is elongated over the span of a month. From the magnitude minimum to the last two points observations in time, the magnitudes are still low relative to the maximum magnitude with a time difference of over approximately 20 days. These traits show an antisymmetry over the total magnitude curve. A verification on the antisymmetric characteristic of a type III variable could be confirmed by magnitude measurements 14 days after the minimum, along with a longer time range. This test would confirm if there exists a magnitude maximum that is not represented by the current sample, and thus exhibiting a symmetric periodicity.

REFERENCES

Cody et al., 2014, Astronomical Journal, volume 147, p. 82

Herbst, W. 2012, Journal of the American Association of Variable Star Observers, 40, 448

Gahm, G. F., Loden. K. Gullbring, E., & Hartstein, D. 1995, A&A, 301, 89

Mathews, G. S., Williams, J. P., & Menard, F. 2012, ApJ, 753, 59

Preibisch & Mamajek, 2008, from the book Handbook of Star Forming Regions, Volume II, ed. B. Reipurth.

Snow, Theodore P., and Theodore P. Snow. Essentials of the Dynamic Universe: An Introduction to Astronomy. St. Paul: West, 1984. Print.